Controlling Product Inhibition through Substrate-Specific Active Sites in Nanoparticle-Based Phosphodiesterase and Esterase

Lan Hu, MD Arifuzzaman, and Yan Zhao*

Department of Chemistry, Iowa State University, Ames, Iowa 50011-3111

ABSTRACT: Hydrolysis of phosphodiester bonds is catalyzed efficiently by DNA- and RNA-hydrolyzing enzymes but their synthetic mimics often fail to display catalytic turnovers because the phosphate products tend to bind the catalytic metal more strongly than the substrates. In this work, we report the direct usage of a phosphate diester substrate as the template and, through micellar imprinting and post-functionalization, created water-soluble nanoparticle catalysts with an active site closely matching the substrate. With a preferential binding for the substrate and a zinc cation in the close proximity of the phosphate, the resulting synthetic phosphodiesterase displayed turnovers one order of magnitude higher than the highest reported previously. The same strategy was used to prepare synthetic esterase with hundreds of turnovers and ability to distinguish closely related substrates.

KEYWORDS: *molecular imprinting, hydrolysis, phosphodiesterase, selectivity, Michaelis-Menten, active site, biomimetic catalysis*

INTRODUCTION

Phosphodiester bonds connect the nucleotides of DNA and RNA into the genetic materials of all life forms. To maintain the integrity of genetic information, these bonds are exceptionally stable in aqueous solution. The half-life for these bonds in DNA, for example, is estimated to be 30 million years at room temperature near neutral pH[1] and that in RNA a few years.[2] Meanwhile, nature frequently needs to manipulate nucleic acids and, therefore, has developed efficient enzymes (i.e., nucleases) that accelerate the hydrolysis, often by 10^{11}–10^{17} times over background hydrolysis.

To better understand the mechanisms of these enzymes and develop useful synthetic catalysts for gene manipulation, chemists have developed[3] and in recent years continue to develop new platforms of artificial phosphodiesterase with novel properties.[4] These studies yielded important insights into the reaction mechanisms and novel structures to mimic the catalytic centers. Some synthetic catalysts could cleave natural nucleic acids under physiological conditions, an important step toward practical biological applications.[5]

A high turnover number for a catalyst translates to a low catalyst loading, a feature very desirable for any catalysts and especially so in biological applications. However, phosphate esters are often bound by their catalytic metal (Zn, Cu, or others) less strongly than their hydrolyzed products, due to the higher negative charge of the latter. Product inhibition thus is prevalent in synthetic phosphodiesterases and often prevents catalytic turnovers completely.[3b-d] It is not uncommon that, in many reported studies, the "catalyst" was used at higher concentrations than the substrate itself. For 2-hydroxypropyl *p*-nitrophenyl phosphate (HPNPP),[3d] a widely used RNA analogue and the primary substrate of the current study, catalytic turnovers were rarely achieved,[6] and the highest reported turnover number (TON) was 5.[6a]

Herein, we report a facile construction of water-soluble nanoparticle phosphodiesterase. With a catalytic active site precisely shaped as the substrate in the hydrophobic core of a cross-linked micelle, our catalyst had a measured TON of >60 for HPNPP. The improvement was derived from a substrate-specific active site that excluded the product due to its different shape, size, and hydrophobicity. The same method also was used to prepare synthetic esterase with hundreds of turnovers and ability to distinguish substrates with minute difference in structure.

RESULTS AND DISCUSSION

The catalysts were prepared through micellar imprinting developed by our group in recent years.[7] Different from other imprinting methods,[8] this technique involved template polymerization within the nanospace of a micelle, using a doubly cross-linkable surfactant such as **1** (Scheme 1). The template-containing micelle was first cross-linked on the surface with diazide **2** by the efficient Cu(I)-catalyzed click reaction and then decorated with a layer of hydrophilic ligand (**3**) by another round of click reaction. Free radical polymerization with DVB solubilized in the micellar core, induced either thermally using AIBN (this work) or photochemically, then "solidified" the core around the template. When performed in the confined nano-

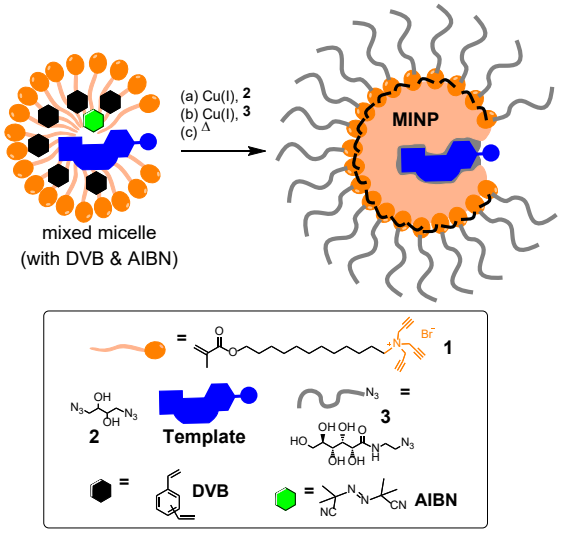

Scheme 1. Preparation of MINP by surface–core double cross-linking of surfactant **1** in the presence of template.

space of a micelle, molecular imprinting has an extraordinary ability to reproduce features of the template in the resulting binding site. Isoleucine and leucine in di- and tripeptides, which are isomers different in the position of a single methyl, were easily distinguished by our molecularly imprinted nanoparticles (MINPs) according to a previous work.[9] Mono- and oligosaccharides different in the stereochemistry of a single hydroxyl could also be differentiated.[10]

Similar to their natural counterparts, synthetic phosphodiesterases commonly use Lewis acidic metals such as zinc to catalyze the hydrolysis.[3-4]Since the phosphate products tend to bind such metals more strongly than the phosphate ester starting materials as mentioned above, it seems inevitable that any metal-based catalysts would suffer product inhibition. However, if the metal–ligand complexation is only *part* of the overall binding and if, by *other noncovalent interactions*, the catalytic active site prefers the substrate over the product, product inhibition should still be avoided and a high TON achieved.

Given the high-fidelity imprinting observed in the cross-linked micelles, the most straightforward way to construct a substrate-selective active site is to *use the substrate itself as the template.* However, such imprinting faces two big challenges. First, for our substrate HPNPP, its complex with zinc is not expected to be stable in our reaction mixture that contains many other neutral and anionic species to compete for the zinc metal—e.g., the bromide counter ion from **1**, ascorbate used in the click reaction, and triazole formed from the click reaction. Second, even if Zn–HPNPP wins in the above competition, the Lewis acidic zinc would hydrolyze the coordinated substrate (precisely as designed), making the imprinting difficult to work.

To overcome these difficulties, we designed and synthesized a photocleavable di-*t*-butylthiouronium derivative (**4**) as a sacrificial functional monomer (FM). Micellar imprinting of complex **4**·HPNPP created MINP$_A$ with the binding site specifically tailored for the substrate itself (Scheme 2). We chose thiouronium **4** because similar (non-photosensitive) FMs were found to bind anionic salts such as carboxylates strongly under our micellar conditions for acidic peptides[11] and very hydrophilic guests such as folic acids.[12]

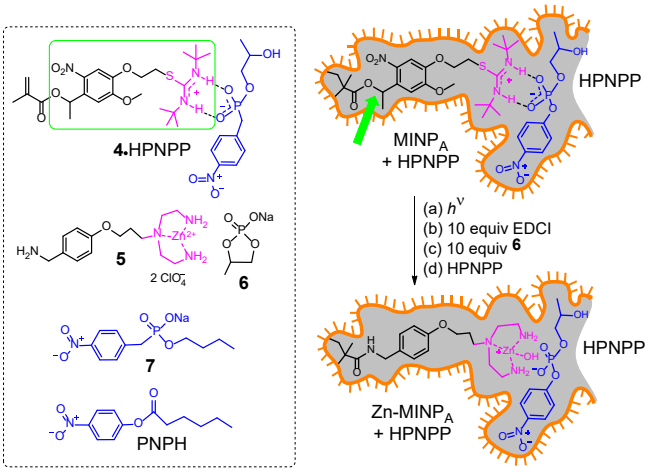

Scheme 2. Structures of molecules and post-modification of MINP$_A$ for HPNPP hydrolysis.

The methacrylate of FM **4** allowed it to be copolymerized into the MINP core whereas its *ortho*-nitrophenyl ester bond can be cleaved cleanly by UV irradiation (indicated by the green arrow in Scheme 2). We have shown that the carboxylic acid group after similar photodeprotection could be activated by N-ethyl-N′-(3-dimethylaminopropyl)carbodiimide hydrochloride (EDCI) and derivatized by amidation.[13] The reactions were facilitated also by the solubility of MINP in organic solvents such as DMF. In this case, zinc-containing amine **5** was used in the amidation: it is similar in dimension to the part of **4** in the green rectangle, with the intention that the catalytic zinc metal would be placed right next to the substrate during the hydrolysis (Scheme 2, lower structure). The hydrolytic product of HPNPP is cyclic phosphate **6**. Even though it has the same metal-binding phosphate, it differs from HPNPP significantly in size, shape, and hydrophobicity. If the imprinting indeed makes the active site highly specific for the substrate, the product should not be able to compete with the substrate for the active site.

Consistent with successful imprinting, MINP$_A$ was found to bind HPNPP with a binding constant (K_a) of $(11.4 \pm 2.5) \times 10^4$ M^{-1} by isothermal titration calorimetry (Table S1 in Supporting Information, entry 1). A closely related compound **7** gave roughly 1/3 of the binding constant (entry 2). Compound **7** can be viewed as the transition-state analogue (TSA) for the hydrolysis of *p*-nitrophenyl hexanoate (PNPH) because it resembles the negatively charged tetrahedral intermediate after the nucleophilic attack of the ester by a hydroxide ion. For comparison, we prepared MINP$_B$ and Zn-MINP$_B$ using **7** as the template, following similar procedures illustrated in Scheme 2. As shown in Table S1 (entries 3 and 4), MINP$_B$ bound its template (**7**) more strongly than HPNPP. Thus, although HPNPP and **7** are quite similar, our micellar imprinting was able to transfer their structural information to the imprinted binding sites to distinguish the two compounds.

To understand the selectivity of the catalysts, we studied the hydrolysis of HPNPP and PNPH by the post-functionalized, Zn-containing MINP$_A$ and MINP$_B$, by monitoring the UV absorption of the phenoxide product at 400 nm in 25 mM HPEPS buffer. Table 1 shows the pseudo-first-order rate constants for the hydrolysis at pH 7.0 at 40 °C. Control experiments indicated that nonimprinted nanoparticles (NINPs) and those without amidation with **6** (i.e., MINP-COOH) were much less active in the catalysis (Figures S8 and S9).

Table 1. Pseudo-first-order rate constants for the hydrolysis of HPNPP and PNPH in 25 mM HEPES buffer (pH 7.0).[a]

Entry	Substrate	k ($\times 10^{-5}$ s^{-1})		
		Zn-MINP$_A$	Zn-MINP$_B$	buffer only
1	HPNPP[b]	1.38 ± 0.06	0.18 ± 0.07	0.023 ± 0.002
2	PNPH[c]	167 ± 14	220 ± 10	0.54 ± 0.01

[a] Reaction rates were measured in 25 mM HEPES buffer (pH 7.0) at 40 °C. [b] [HPNPP] = 100 μM. [MINP$_A$] = 5.0 μM. [c] [PNPH] = 40 μM. [MINP$_B$] = 8.0 μM.

Table 2. Michaelis-Menten parameters of the Zn-MINPs for its substrate.[a]

Entry	catalyst	substrate	pH	V_{max} (mM/s) ($\times 10^{-4}$)	K_m (mM)	k_{cat} (s^{-1}) ($\times 10^{-3}$)	k_{cat}/K_m ($M^{-1}\,s^{-1}$)
1	Zn-MINP$_A$	HPNPP	7.0	0.015 ± 0.001	0.77 ± 0.02	0.61 ± 0.01	0.80
2	Zn-MINP$_B$	PNPH	7.0	3.27 ± 0.05	0.76 ± 0.08	36.7 ± 4.80	48.0
3	Zn-MINP$_B$	PNPH	7.5	2.21 ± 0.04	0.36 ± 0.04	27.6 ± 1.81	77.0
4	Zn-MINP$_B$	PNPH	8.0	1.94 ± 0.22	0.20 ±0.04	23.9 ± 2.10	120
5	Zn-MINP$_B$	PNPH	8.5	1.72 ± 0.04	0.12 ± 0.01	21.3 ± 0.45	178
6	Zn-MINP$_B$	PNPH	9.0	7.03 ± 0.22	0.41 ± 0.01	87.7 ± 2.43	213
7	Zn-MINP$_B$	PNPH	9.5	17.8 ± 0.91	0.89 ± 0.02	220 ± 10.0	247

[a] The hydrolysis of HPNPP was catalyzed by [Zn-MINP$_A$] in 25 mM HEPES buffer at 40 °C. [Zn-MINP$_A$] = 8.0 μM. The hydrolysis of PNPH was catalyzed by [Zn-MINP$_B$] in 25 mM HEPES buffer at 40 °C. [Zn-MINP$_B$] = 8.0 μM.

Table 1 shows that our micellar imprinting/post-functionalization indeed was able to transfer the structural information of the templates to the final catalysts. Zn-MINP$_A$, designed for HPNPP, was ca. 8 times more active than Zn-MINP$_B$ in the hydrolysis of HPNPP (entry 1). Likewise, Zn- MINP$_B$, designed for PNPH, was more active than Zn-MINP$_A$ in the hydrolysis of PNPH, except the improvement was more modest (entry 2). The most likely reason for the smaller difference in the PNPH hydrolysis was the much higher intrinsic reactivity the substrate in comparison to HPNPP (see the corresponding background reaction rates in Table 1). Generally speaking, the more reactive a substrate, the more it can tolerate an imperfect catalyst.[14]

In agreement with our catalytic designs, both catalysts displayed enzyme-like Michaelis-Menten kinetics. Zn-MINP$_A$ afforded a K_m value of 0.77 mM and k_{cat} of 0.61×10^{-3} s^{-1} at pH 7 (Table 2, entry 1). With the background rate constant (k_{uncat}) measured at 0.023×10^{-5} s^{-1} (Table 1), the rate acceleration factor (k_{cat}/k_{uncat}) was about 2700. The catalytic efficiency (k_{cat}/K_m) of Zn-MINP$_A$ was 0.80 $M^{-1}s^{-1}$ at pH 7, comparable to many synthetic di- or tri-nuclear zinc catalysts under similar conditions,[3b] despite the mononuclear nature of our catalyst.

Hydrolysis of PNPH by Zn-MINP$_B$ was significantly faster, with K_m = 0.76 mM and k_{cat} = 36.7×10^{-3} s^{-1} at pH 7 (entry 2). The catalytic efficiency (k_{cat}/K_m) is 48.0 M^{-1} s^{-1}, higher than those of most zinc-based synthetic esterases for *p*-nitrophenyl esters[15] including our own reported previously.[16]

Zinc catalyzes hydrolysis of esters typically by the metal-bound hydroxide,[3] as shown in the proposed mechanisms (Scheme 3). Figure 1 shows pH dependence of the hydrolysis of PNPH by Zn-MINP$_B$ and the profile resembled those for peptide-based artificial zinc esterases reported in the literature.[15] The sigmoidal curve is normally considered to come from a single protonation/deprotonation step for the metal-bound water that acts as the nucleophile in the hydrolysis. Nonlinear least squares curve fitting yielded a pK_a of 7.89 ± 0.25. The number is slightly higher than those for zinc-bound water in natural zinc enzymes (6.8–7.3 for carbonic anhydrase B and C)[17] and lower than those of other artificial zinc esterases based on folded/self-assembled peptides.[15] For the HPNPP hydrolysis, Zn-MINP$_A$ showed a very similar pH profile, affording a pK_a of 7.87 ± 0.25 (Figure S18). Thus, no matter what the metal-bound hydroxide attacked, the carbonyl of PNPH or the β hydroxyl of HPNPP, the pH response of the MINP catalysts reflected the same protonation/deprotonation step.

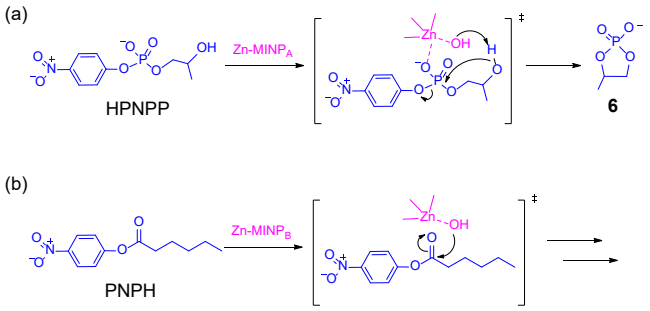

Scheme 3. Proposed mechanism for the MINP-catalyzed hydrolysis of (a) HPNPP and (b) PNPH.

Whether for phosphate or carboxylic acid esters, the hydrolyzed products tend to have stronger binding for the zinc metal than the starting materials. Thus, synthetic enzymes to hydrolyze these compounds frequently suffer from strong product inhibition.[3d,15b] The highest reported TON for HPNPP in the literature was 5[6a] as mentioned above and that for *p*-nitrophenyl esters with peptide-based artificial zinc esterases was 50.[15a]

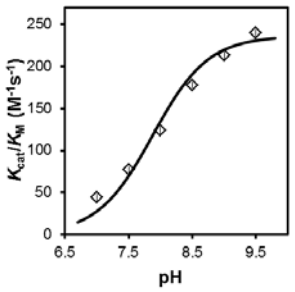

Figure 1. pH dependence of the hydrolysis of PNPH by Zn-MINP$_B$. The smooth curve was obtained by nonlinear least-squares curve fitting to the equation, $k_{cat}/K_m = (k_{cat}/K_m)_{max} \times 10^{-pKa}/(10^{-pH} + 10^{-pKa})$, with the inflection point corresponding to the pK_a of the zinc-bound water (7.89 ± 0.25).[15e]

Figure 2a shows the amount of product (*p*-nitrophenoxide) formed as a function of time in HPNPP hydrolysis catalyzed by Zn-

$MINP_A$. With a 1 mol % catalyst loading, the maximum TON obtainable for the experiment was 100. After 600 min, the reaction reached 61%, thus giving a TON of 61. For PNPH, we used a 0.2 mol % catalyst loading because the reaction was much faster. After 300 min, the TON was 300 for Zn-$MINP_B$. Thus, both MINPs displayed a much higher turnover number than previously reported catalysts constructed on different platforms. The results suggest that a substrate-specific active site indeed can block more strongly coordinating products from entering the active site.

Another conceivable benefit of a catalyst with a substrate-specific active site is their selectivity for the very substrate they are designed for. Because the catalytic metal resides in the active site, substrates that fit poorly should be excluded and display low reactivity. To test this hypothesis, we studied the competitive hydrolysis of PNPH and *p*-nitrophenyl butyrate (PNPB) by Zn-$MINP_B$ for the easy synthesis of the substrates. Although PNPB should fit within the active site of MINP imprinted from **7**, its shorter acyl chain could not displace all the "high-energy" water molecules inside the hydrophobic active site, weakening the binding consequently. Generally speaking, putting water molecules in a hydrophobic microenvironment is unfavorable, especially if they are confined.[18] The entropic cost of trapping water molecules can be as high as 2 kcal/mol in some cases for a single water molecule.[19]

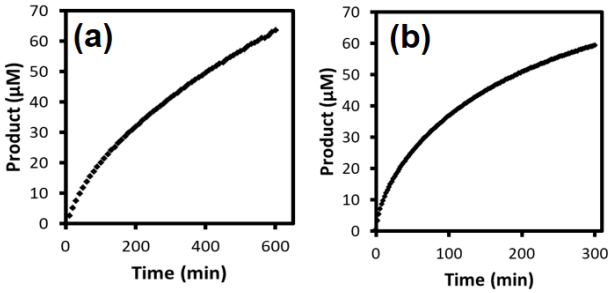

Figure 2. Amount of *p*-nitrophenoxide formed as a function of time, calculated based on an extinction coefficient of $\varepsilon_{400} = 0.0216\ \mu M^{-1}\ cm^{-1}$. (a) The turnover number of 61 was obtained at 600 min. HPNPP (100 μM) in a 25 mM HEPES buffer (pH 8.0) at 60 °C, in the presence of 1 μM Zn-$MINP_A$. (b) The turnover number of 300 was obtained at 300 min. PNPH (100 μM) in a 25 mM HEPES buffer (pH 8.0) at 40 °C, in the presence of 0.2 μM Zn-$MINP_B$.

As shown by the data points in open circles (○) in Figure 3, 40 μM PNPB hydrolyzed rather slowly in the presence of 8 μM Zn-$MINP_B$, evident from the small increase of absorbance at 400 nm from *p*-nitrophenoxide. When another batch of 40 μM PNPB was added at 15 min, the reaction rate increased slightly (△), due to the higher total concentration of the substrate in the solution. When 40 μM PNPH was added at 15 min instead (□), release of *p*-nitrophenoxide was much faster. Thus, as designed, Zn-$MINP_B$ was able to select its preferred substrate (PNPH) from the mixture, despite the identical reactive group and very similar structures.

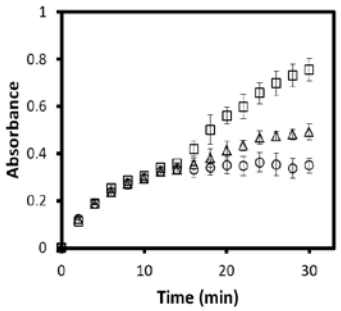

Figure 3. Absorbance at 400 nm as a function of time for the hydrolysis of 40 μM 4-nitrophenyl butyrate (**9**) catalyzed by Zn-MINP(**4a**) in a 25 mM HEPES buffer (pH 7.0) at 40 °C (○). In the data series marked with triangles (△), 40 μM PNPB was added at 15 min. In the data series marked with squares (□), 40 μM PNPH was added again at 15 min. [MINP(**4a**)] = 8 μM.

CONCLUSIONS

With molecular imprinting, we could use the TSA of a reaction or even the substrate directly as the template, to create binding sites inside water-soluble cross-linked micelles highly specific for the substrate. Solubility of these molecularly imprinted nanoparticles in organic solvent such as DMF allowed us to manipulate the binding site through standard chemistry, to swap the binding group with the catalytic group. Because the binding and catalytic groups had similar dimensions, the catalytic group was placed right next to the bond that needed to be transformed, making it possible for our mononuclear zinc catalyst with simple ligand structures to approach previously reported di- and trinuclear zinc catalysts in catalytic efficiency. More importantly, turnover numbers unachievable by previous systems could be easily obtained in our imprinted catalysts, whether to hydrolyze phosphate or carboxylic acid esters. These results give us hope that, with more advanced catalytic features, efficient and selective catalysts that mimic natural enzymes can be prepared in the future, and find many applicants in chemistry and biology.

AUTHOR INFORMATION

Corresponding Author

*E-mail for Y.Z.: zhaoy@iastate.edu

Notes

The authors declare no competing financial interests.

Supporting Information

Experimental details, ITC titration curves, Michaelis-Menten data, and additional figures. This material is available free of charge via the Internet at http://pubs.acs.org.

ACKNOWLEDGMENT

We thank NSF (CHE-1708526) for financial support of this research.

REFERENCES

1. Schroeder, G. K.; Lad, C.; Wyman, P.; Williams, N. H.; Wolfenden, R. The Time Required for Water Attack at the Phosphorus Atom of Simple Phosphodiesters and of DNA. *Proc. Natl. Acad. Sci. U. S. A.* **2006**, *103*, 4052-4055.

2. Thompson, J. E.; Kutateladze, T. G.; Schuster, M. C.; Venegas, F. D.; Messmore, J. M.; Raines, R. T. Limits to Catalysis by Ribonuclease A. *Bioorg. Chem.* **1995**, *23*, 471-481.
3. (a) Lonnberg, H. Cleavage of Rna Phosphodiester Bonds by Small Molecular Entities: A Mechanistic Insight. *Org. Biomol. Chem.* **2011**, *9*, 1687-1703. (b) Desbouis, D.; Troitsky, I. P.; Belousoff, M. J.; Spiccia, L.; Graham, B. Copper(Ii), Zinc(Ii) and Nickel(Ii) Complexes as Nuclease Mimetics. *Coord. Chem. Rev.* **2012**, *256*, 897-937. (c) Mancin, F.; Scrimin, P.; Tecilla, P. Progress in Artificial Metallonucleases. *Chem. Commun.* **2012**, *48*, 5545-5559. (d) Mikkola, S.; Lonnberg, T.; Lonnberg, H. Phosphodiester Models for Cleavage of Nucleic Acids. *Beilstein J. Org. Chem.* **2018**, *14*, 803-837.
4. (a) Manea, F.; Houillon, F. B.; Pasquato, L.; Scrimin, P. Nanozymes: Gold-Nanoparticle-Based Transphosphorylation Catalysts. *Angew. Chem. Int. Ed.* **2004**, *43*, 6165-6169. (b) Martin, M.; Manea, F.; Fiammengo, R.; Prins, L. J.; Pasquato, L.; Scrimin, P. Metallodendrimers as Transphosphorylation Catalysts. *J. Am. Chem. Soc.* **2007**, *129*, 6982-6983. (c) Gruber, B.; Kataev, E.; Aschenbrenner, J.; Stadlbauer, S.; König, B. Vesicles and Micelles from Amphiphilic Zinc(Ii)–Cyclen Complexes as Highly Potent Promoters of Hydrolytic DNA Cleavage. *J. Am. Chem. Soc.* **2011**, *133*, 20704-20707. (d) Tirel, E. Y.; Bellamy, Z.; Adams, H.; Lebrun, V.; Duarte, F.; Williams, N. H. Catalytic Zinc Complexes for Phosphate Diester Hydrolysis. *Angew. Chem. Int. Ed.* **2014**, *53*, 8246-8250. (e) Savelli, C.; Salvio, R. Guanidine-Based Polymer Brushes Grafted onto Silica Nanoparticles as Efficient Artificial Phosphodiesterases. *Chem. -Eur. J.* **2015**, *21*, 5856-5863. (f) Chen, J. L.-Y.; Pezzato, C.; Scrimin, P.; Prins, L. J. Chiral Nanozymes–Gold Nanoparticle-Based Transphosphorylation Catalysts Capable of Enantiomeric Discrimination. *Chem.-Eur. J.* **2016**, *22*, 7028-7032. (g) Bím, D.; Svobodová, E.; Eigner, V.; Rulíšek, L.; Hodačová, J. Copper(Ii) and Zinc(Ii) Complexes of Conformationally Constrained Polyazamacrocycles as Efficient Catalysts for Rna Model Substrate Cleavage in Aqueous Solution at Physiological Ph. *Chem. -Eur. J.* **2016**, *22*, 10426-10437. (h) della Sala, F.; Chen, J. L. Y.; Ranallo, S.; Badocco, D.; Pastore, P.; Ricci, F.; Prins, L. J. Reversible Electrochemical Modulation of a Catalytic Nanosystem. *Angew. Chem. Int. Ed.* **2016**, *55*, 10737-10740. (i) Neri, S.; Martin, S. G.; Pezzato, C.; Prins, L. J. Photoswitchable Catalysis by a Nanozyme Mediated by a Light-Sensitive Cofactor. *J. Am. Chem. Soc.* **2017**, *139*, 1794-1797.
5. (a) Matsuda, S.; Ishikubo, A.; Kuzuya, A.; Yashiro, M.; Komiyama, M. Conjugates of a Dinuclear Zinc(Ii) Complex and DNA Oligomers as Novel Sequence-Selective Artificial Ribonucleases. *Angew. Chem. Int. Ed.* **1998**, *37*, 3284-3286. (b) Morrow, J. R.; Iranzo, O. Synthetic Metallonucleases for Rna Cleavage. *Curr. Opin. Chem. Biol.* **2004**, *8*, 192-200. (c) Murtola, M.; Wenska, M.; Stromberg, R. Pnazymes That Are Artificial Rna Restriction Enzymes. *J. Am. Chem. Soc.* **2010**, *132*, 8984-8990. (d) Yu, Z.; Cowan, J. A. Metal Complexes Promoting Catalytic Cleavage of Nucleic Acids—Biochemical Tools and Therapeutics. *Curr. Opin. Chem. Biol.* **2018**, *43*, 37-42.
6. (a) Feng, G.; Natale, D.; Prabaharan, R.; Mareque-Rivas, J. C.; Williams, N. H. Efficient Phosphodiester Binding and Cleavage by a Zn^{ii} Complex Combining Hydrogen-Bonding Interactions and Double Lewis Acid Activation. *Angew. Chem. Int. Ed.* **2006**, *45*, 7056-7059. (b) Avenier, F.; Hollfelder, F. Combining Medium Effects and Cofactor Catalysis: Metal-Coordinated Synzymes Accelerate Phosphate Transfer by 108. *Chem.-Eur. J.* **2009**, *15*, 12371-12380.
7. Awino, J. K.; Zhao, Y. Protein-Mimetic, Molecularly Imprinted Nanoparticles for Selective Binding of Bile Salt Derivatives in Water. *J. Am. Chem. Soc.* **2013**, *135*, 12552-12555.
8. (a) Wulff, G. Enzyme-Like Catalysis by Molecularly Imprinted Polymers. *Chem. Rev.* **2001**, *102*, 1-28. (b) Haupt, K.; Mosbach, K. Molecularly Imprinted Polymers and Their Use in Biomimetic Sensors. *Chem. Rev.* **2000**, *100*, 2495-2504. (c) Lakshmi, D.; Bossi, A.; Whitcombe, M. J.; Chianella, I.; Fowler, S. A.; Subrahmanyam, S.; Piletska, E. V.; Piletsky, S. A. Electrochemical Sensor for Catechol and Dopamine Based on a Catalytic Molecularly Imprinted Polymer-Conducting Polymer Hybrid Recognition Element. *Anal. Chem.* **2009**, *81*, 3576-3584. (d) Shinde, S.; El-Schich, Z.; Malakpour, A.; Wan, W.; Dizeyi, N.; Mohammadi, R.; Rurack, K.; Gjörloff Wingren, A.; Sellergren, B. Sialic Acid-Imprinted Fluorescent Core–Shell Particles for Selective Labeling of Cell Surface Glycans. *J. Am. Chem. Soc.* **2015**, *137*, 13908-13912. (e) Liu, J.; Yin, D.; Wang, S.; Chen, H. Y.; Liu, Z. Probing Low-Copy-Number Proteins in a Single Living Cell. *Angew. Chem. Int. Ed.* **2016**, *55*, 13215-13218. (f) Horikawa, R.; Sunayama, H.; Kitayama, Y.; Takano, E.; Takeuchi, T. A Programmable Signaling Molecular Recognition Nanocavity Prepared by Molecular Imprinting and Post-Imprinting Modifications. *Angew. Chem. Int. Ed.* **2016**, *55*, 13023-13027. (g) Panagiotopoulou, M.; Salinas, Y.; Beyazit, S.; Kunath, S.; Duma, L.; Prost, E.; Mayes, A. G.; Resmini, M.; Bui, B. T. S.; Haupt, K. Molecularly Imprinted Polymer Coated Quantum Dots for Multiplexed Cell Targeting and Imaging. *Angew. Chem. Int. Ed.* **2016**, *55*, 8244-8248. (h) Shen, X.; Huang, C.; Shinde, S.; Jagadeesan, K. K.; Ekström, S.; Fritz, E.; Sellergren, B. Catalytic Formation of Disulfide Bonds in Peptides by Molecularly Imprinted Microgels at Oil/Water Interfaces. *ACS Appl. Mater. Interfaces* **2016**, *8*, 30484-30491. (i) Bertolla, M.; Cenci, L.; Anesi, A.; Ambrosi, E.; Tagliaro, F.; Vanzetti, L.; Guella, G.; Bossi, A. M. Solvent-Responsive Molecularly Imprinted Nanogels for Targeted Protein Analysis in Maldi-Tof Mass Spectrometry. *ACS Appl. Mater. Interfaces* **2017**, *9*, 6908-6915. (j) Jiang, L.; Messing, M. E.; Ye, L. Temperature and Ph Dual-Responsive Core-Brush Nanocomposite for Enrichment of Glycoproteins. *ACS Appl. Mater. Interfaces* **2017**, *9*, 8985-8995.
9. Awino, J. K.; Gunasekara, R. W.; Zhao, Y. Sequence-Selective Binding of Oligopeptides in Water through Hydrophobic Coding. *J. Am. Chem. Soc.* **2017**, *139*, 2188-2191.
10. (a) Awino, J. K.; Gunasekara, R. W.; Zhao, Y. Selective Recognition of D-Aldohexoses in Water by Boronic Acid-Functionalized, Molecularly Imprinted Cross-Linked Micelles. *J. Am. Chem. Soc.* **2016**, *138*, 9759-9762. (b) Gunasekara, R. W.; Zhao, Y. A General Method for Selective Recognition of Monosaccharides and Oligosaccharides in Water. *J. Am. Chem. Soc.* **2017**, *139*, 829-835.
11. Fa, S.; Zhao, Y. Water-Soluble Nanoparticle Receptors Supramolecularly Coded for Acidic Peptides. *Chem. -Eur. J.* **2018**, *24*, 150-158.
12. Duan, L.; Zhao, Y. Selective Binding of Folic Acid and Derivatives by Imprinted Nanoparticle Receptors in Water. *Bioconjugate Chem.* **2018**, *29*, 1438-1445.
13. Awino, J. K.; Zhao, Y. Water-Soluble Molecularly Imprinted Nanoparticles (Minps) with Tailored, Functionalized, Modifiable Binding Pockets. *Chem.-Eur. J.* **2015**, *21*, 655-661.
14. Menger, F. M.; Ladika, M. Origin of Rate Accelerations in an Enzyme Model: The P-Nitrophenyl Ester Syndrome. *J. Am. Chem. Soc.* **1987**, *109*, 3145-3146.
15. (a) Der, B. S.; Edwards, D. R.; Kuhlman, B. Catalysis by a De Novo Zinc-Mediated Protein Interface: Implications for Natural Enzyme Evolution and Rational Enzyme Engineering. *Biochemistry* **2012**, *51*, 3933-3940. (b) Zastrow, M. L.; Peacock, A. F. A.; Stuckey, J. A.; Pecoraro, V. L. Hydrolytic Catalysis and Structural Stabilization in a Designed Metalloprotein. *Nat. Chem.* **2012**, *4*, 118-123. (c) Zastrow, M. L.; Pecoraro, V. L. Influence of Active Site Location on Catalytic Activity in De Novo-Designed Zinc Metalloenzymes. *J. Am. Chem. Soc.* **2013**, *135*, 5895-5903. (d) Song, W. J.; Tezcan, F. A. A Designed Supramolecular Protein Assembly with in Vivo Enzymatic Activity. *Science* **2014**, *346*, 1525-1528. (e) Rufo, C. M.; Moroz, Y. S.; Moroz, O. V.; Stohr, J.; Smith, T. A.; Hu, X. Z.; DeGrado, W. F.; Korendovych, I. V. Short Peptides Self-Assemble to Produce Catalytic Amyloids. *Nat. Chem.* **2014**, *6*, 303-309. (f) Burton, A. J.; Thomson, A. R.; Dawson, W. M.; Brady, R. L.; Woolfson, D. N. Installing Hydrolytic Activity into a Completely De Novo Protein Framework. *Nat. Chem.* **2016**, *8*, 837-844.
16. Arifuzzaman, M.; Zhao, Y. Artificial Zinc Enzymes with Fine-Tuned Catalytic Active Sites for Highly Selective Hydrolysis of Activated Esters. *Acs Catal* **2018**, *8*, 8154-8161.
17. Verpoorte, J. A.; Mehta, S.; Edsall, J. T. Esterase Activities of Human Carbonic Anhydrases B and C. *J. Biol. Chem.* **1967**, *242*, 4221-4229.
18. Awino, J. K.; Hu, L.; Zhao, Y. Molecularly Responsive Binding through Co-Occupation of Binding Space: A Lock–Key Story. *Org. Lett.* **2016**, *18*, 1650-1653.
19. Dunitz, J. D. The Entropic Cost of Bound Water in Crystals and Biomolecules. *Science* **1994**, *264*, 670.

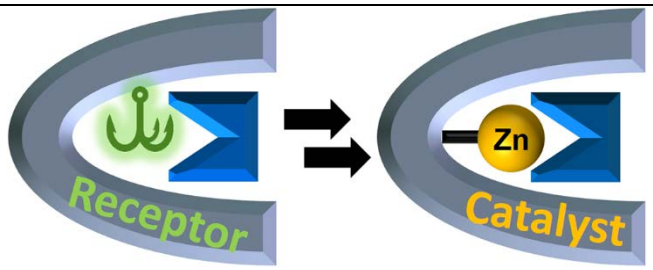
Receptor
Zn
Catalyst